Senescence-Associated Exosome Release from Human Prostate Cancer Cells

Brian D. Lehmann,[1] Matthew S. Paine,[1] Adam M. Brooks,[1] James A. McCubrey,[2,3] Randall H. Renegar,[1] Rong Wang,[1] and David M. Terrian[1,3]

Departments of [1]Anatomy and Cell Biology and [2]Microbiology and Immunology, and [3]Leo W. Jenkins Cancer Center, Brody School of Medicine, East Carolina University, Greenville, North Carolina

Abstract

Males of advanced age represent a rapidly growing population at risk for prostate cancer. In the contemporary setting of earlier detection, a majority of prostate carcinomas are still clinically localized and often treated using radiation therapy. Our recent studies have shown that premature cellular senescence, rather than apoptosis, accounts for most of the clonogenic death induced by clinically relevant doses of irradiation in prostate cancer cells. We show here that this treatment-induced senescence was associated with a significantly increased release of exosome-like microvesicles. In premature senescence, this novel secretory phenotype was dependent on the activation of p53. In addition, the release of exosome-like microvesicles also increased during proliferative senescence in normal human diploid fibroblasts. These data support the hypothesis that senescence, initiated either by telomere attrition (e.g., aging) or DNA damage (e.g., radiotherapy), may induce a p53-dependent increase in the biogenesis of exosome-like vesicles. Ultrastructural analysis and RNA interference–mediated knockdown of Tsg101 provided significant evidence that the additional exosomes released by prematurely senescent prostate cancer cells were principally derived from multivesicular endosomes. Moreover, these exosomes were enriched in B7-H3 protein, a recently identified diagnostic marker for prostate cancer, and an abundance of what has recently been termed "exosomal shuttle RNA." Our findings are consistent with the proposal that exosomes can transfer cargos, with both immunoregulatory potential and genetic information, between cells through a novel mechanism that may be recruited to increase exosome release during accelerated and replicative cellular senescence. [Cancer Res 2008;68(19):7864–71]

Introduction

Advanced age is the dominant risk factor for developing carcinoma of the prostate. The incidence of prostate cancer increases dramatically in men beyond 50 years of age and reaches a frequency of one-in-seven between ages 60 and 79 years (1). Once a prostatic intraepithelial neoplasia has been initiated, a host of age-related alterations have the potential to influence the evolution and growth of malignant lesions; including chronic oxidative stress and inflammation, genomic instability, a loss of immune surveillance and telomere attrition. Telomere attrition limits the reproductive life span of normal human cells by inducing a permanent cell cycle arrest that is termed replicative senescence (2). Although replicative senescence is generally considered a natural tumor suppressor mechanism, owing to its antiproliferative effects, there is now evidence that senescent prostate fibroblasts populating aged tissue may secrete soluble growth factors capable of altering the host microenvironment (3). Understanding the relationships between biological aging, this "senescent secretory phenotype," and age-related diseases such as prostate cancer represents an emerging area of active research.

Although no longer dividing, senescent fibroblasts remain metabolically active and secrete high levels of epithelial growth factors and matrix metalloproteinases (4–8). Thus, an accumulation of senescent fibroblasts can alter the surrounding microenvironment; the so-called "reactive stroma" associated with some carcinomas, and promote the growth and tumor progression of initiated human prostate epithelial cells (9). The factors secreted by senescent cells vary depending on cell type and the vast majority of studies to date have analyzed this senescent secretory phenotype using normal fibroblasts that have reached replicative exhaustion as a cell model (4–9). These studies have convincingly shown that the p53, $p21^{WAF1/Cip1}$ (p21), $p16^{INK4a}$ (p16), and pRb tumor suppressors are important senescence regulators (10). The functional collaboration between the p16/pRb and p53/p21 pathways responsible for initiating a permanent growth arrest have been described in detail (11, 12), yet we still understand little about the age-related mechanisms involved in initiating or maintaining the senescent secretory phenotype.

External beam radiation has long been one of the major curative treatment options for patients with clinically localized prostate cancer. We have recently presented evidence that the *in vitro* effectiveness of this treatment modality may be principally attributed to its ability to induce a p53-dependent terminal growth arrest, termed accelerated or "premature senescence," rather than a direct cell kill (13). There is no direct evidence that the clinical use of irradiation induces premature senescence in prostate tumor cells *in vivo*. However, there is evidence that chemotherapeutics and irradiation selectively induce premature senescence within the malignant foci of breast cancer specimens (14).

Much recent attention has been focused on the task of identifying soluble factors secreted by senescent fibroblasts and tumor cells and in characterizing their paracrine activities (3–8, 15). It is important to note, however, that in addition to soluble paracrine factors, many tumor cells also release microvesicles that have been termed "exosomes" (16). Exosomes are small, cup-shaped, vesicles of ~100 nm diameter that are initially formed within the endosomal compartment and are secreted when a multivesicular endosome (MVE) fuses with the plasma membrane (17, 18). Interestingly, the abundance of exosomes released generally correlates positively with advanced stages of cancer

Requests for reprints: David M. Terrian, Department of Anatomy and Cell Biology, Brody School of Medicine, East Carolina University, 600 Moye Boulevard, Greenville, NC 27834. Phone: 252-744-3247; Fax: 252-744-2850; E-mail: terriand@ecu.edu.

doi:10.1158/0008-5472.CAN-07-6538

progression (16). Moreover, there is recent evidence that the irradiation-induced activation of p53 has the potential to increase exosome release from nonquiescent human lung cancer cells (19).

In the present study, we sought to determine whether a relationship exists between the irradiation-induced activation of p53, premature cellular senescence and alterations in exosome biogenesis in human prostate cancer cells. We compared presenescent (i.e., mock-irradiated) and senescent (irradiated) prostate cancer cells for alterations in the senescence-associated secretion of exosome-like particles. This analysis identified a novel and previously unrecognized connection between the induction of p53-dependent senescence and the release of endosome-derived exosomes in human prostate cancer cells. Moreover, our analysis of replicative senescence in normal human fibroblasts provided preliminary evidence of a more general functional relationship that may be intrinsic to this mode of clonogenic death. Importantly, the results of our biochemical analyses also support the concept that senescence-associated exosomes can transfer cargos, with both immunoregulatory potential and genetic information, between cells through a novel mechanism that may be recruited to increase exosome release during cellular senescence.

Materials and Methods

Cell Culture

LNCaP, 22Rv1, and DU145 cells were acquired from the American Type Culture Collection (ATCC CRL-1740, CRL-2505, and HTB-81, respectively). LNCaP and 22Rv1 cultures were maintained in RPMI 1640 medium containing 2 mmol/L of L-glutamine, 10 mmol/L of HEPES, 1 mmol/L of sodium pyruvate, 4.5 g/L of glucose, and 1.5 g/L of sodium bicarbonate, supplemented with 10% fetal bovine serum (FBS), 100 units/mL of penicillin and 100 mg/mL of streptomycin. The effects of p53 inactivation on irradiation-induced cellular senescence and exosome release were examined by infecting LNCaP and 22Rv1 cells with a retroviral vector encoding dominant negative (DN) p53 as described previously (13).

DU145 cells were cultured in MEM with 2 mmol/L of L-glutamine and Earle's balanced salt solution adjusted to contain 1.5 g/L of sodium bicarbonate, 0.1 mmol/L of nonessential amino acids, 0.1 mmol/L of sodium pyruvate, supplemented with 10% FBS and 100 units/mL of penicillin and 100 mg/mL of streptomycin. Normal human dermal fibroblasts (NHDF) were obtained from Dr. Warren Knudson (Department of Anatomy and Cell Biology, East Carolina University, Greenville, NC) and were grown as an adherent culture with MEM containing 2 mmol/L of L-glutamine and Earle's balanced salt solution adjusted to contain 1.5 g/L of sodium bicarbonate, 0.1 mmol/L of nonessential amino acids, 0.1 mmol/L of sodium pyruvate, supplemented with 10% FBS and 100 units/mL of penicillin and 100 mg/mL of streptomycin.

Senescence Induction

Accelerated senescence. Subconfluent cultures of human prostate cancer cells (LNCaP, 22Rv1, and DU145) were routinely seeded in triplicate and allowed to proliferate to ~70% confluence prior to mock-irradiation (0 Gy) or exposure to an irradiation dose of 4 Gy, using a Gammacell 40 (Atomic Energy of Canada Limited) Cs^{137} source. After treatment, the cells were left to recover for 4 days in complete medium. At this time postirradiation, a majority of LNCaP and 22Rv1, but not DU145, cells test positive for various phenotypic markers of cellular senescence (13) and could be used for comparisons of exosome release from presenescent (mock-irradiated) versus prematurely senescent (irradiated) cells.

Replicative senescence. To establish cells at replicative senescence, NHDF cells were cultured until cell doubling time exceeded 12 days (>10 cell doublings). At this time, the cells were considered to have reached replicative exhaustion. Induction of senescence was routinely verified by measuring the increased senescence-associated β-galactosidase (SA β-Gal) activity, as described previously (13).

Exosome Purification and Analysis

Exosomes were isolated from medium conditioned by LNCaP, 22Rv1, and DU145 cells using the differential centrifugation protocol of Thery and colleagues (20), with the following modifications. Subconfluent cultures were washed twice in PBS and incubated for 48 h in serum-free medium. In our studies of irradiation-induced senescence, this period of conditioning was initiated 4 days after a single exposure to either 0 or 4 Gy. This conditioned medium was decanted, centrifuged at 500 × *g* for 10 min to sediment cells and at 14,000 × *g* for 15 min to eliminate cell debris. Exosomes were sedimented by ultracentrifugation at 100,000 × *g* for 70 min and the resultant pellets were washed once in PBS. The washed pellets were examined by electron microscopy (see below) and examined for their protein or lipid content using SDS-PAGE and Daiichi silver staining, immunoblotting, or stained using Vybrant DiI (Molecular Probes), a fluorescent carbocyanine lipid analogue that uniformly stains biological membranes (21). For lipid staining, equal aliquots of the final exosome suspensions were incubated for 20 min at 37°C in the presence of 5 μmol/L of DiI and excess dye was removed by washing in PBS. The fluorescent intensity (Ex^{530}, Em^{590}) of these DiI-stained membrane fractions were measured using a Synergy HT microplate reader (Bio-Tek) and used for comparisons of vesicle secretion. All values were corrected for differences in the total number of viable cells left on the plate after the 48-h conditioning period, and then measured using the trypan blue exclusion assay.

Electron Microscopy

Exosome preparations from LNCaP and 22Rv1 cells were mixed with equal quantities of freshly prepared 4% paraformaldehyde and 5 μL of the sample was loaded onto carbon-coated formvar grids. After incubation in a moist atmosphere for 20 min, the samples were washed thrice in PBS and then fixed for 5 min in 1% glutaraldehyde. After three washes, the exosome samples were stained for 10 min with saturated aqueous uranyl. Exosomes were examined with a JEOL 1200EX electron microscope at 60 kV.

Western Blot Analysis

Immunoblots were performed as described previously (13). Antibodies purchased from R&D Systems were raised against human B7-H3. Anti-Tsg101 antibody (C-2) was purchased from Santa Cruz Biotechnology. Anti–β-actin antibody (Ab-1) was purchased from Calbiochem. Where specified, the relative intensity of immunospecific bands were analyzed with a Molecular Dynamics densitometer and ImageQuant software (GE Healthcare).

RNA Interference

22Rv1 cells were transfected with oligomer-Lipofectamine 2000 complexes using 100 nmol/L of human Tsg101 SMARTpool small interfering RNAs (siRNA; NM_006292) or a nontargeting siRNA control, according to the manufacturer's protocol (Dharmacon, Inc.). Briefly, 3 days after cells had either been mock-irradiated or exposed to a 4 Gy dose, the cultures were washed with PBS and incubated for 24 h in serum-free medium. 22Rv1 cells were then incubated for 24 h in the presence of 100 nmol/L of siRNA-Lipofectamine complexes before the medium was replaced with serum- and siRNA-free medium. After 72 h, the conditioned medium was removed for exosome purification and cell lysates were prepared using the corresponding adherent cells.

Total RNA Extraction and Analysis

Exosome fractions were resuspended in RNase-free water, briefly sonicated, and total nucleic acid was extracted using TRIzol reagent, according to the manufacturer's protocol (Invitrogen Corp.). RNA precipitates were resuspended in RNase-free PBS and divided into three equal aliquots. Control samples were incubated for 10 min at 37°C, whereas the remaining two were incubated, under identical conditions, in the presence of either 0.4 μg/μL of RNase or 0.083 units/μL of DNase. These samples were separated on 2% agarose gels and stained with ethidium bromide.

Analysis of Clonogenic Survival and Cell Fate

Assays of clonogenic survival after a single exposure to 2 Gy (SF_2), apoptosis (i.e., TdT-mediated dUTP nick end labeling, flow cytometric analysis of DNA content, and acridine orange/ethidium bromide staining), and cellular senescence (SA β-Gal and carboxyfluorescein diacetate succinimidyl ester flow cytometry) were performed as previously described (13).

Data Analysis

Values shown are representative of triplicate determinations in two or more experiments, unless otherwise specified, and treatment effects were evaluated using a two-sided Student's *t* test. Errors are SE of averaged results and $P < 0.05$ values were taken as a significant difference between means.

Results and Discussion

The three primary responses mediated by p53 in response to irradiation-induced DNA damage are cell cycle arrest, apoptosis, or cellular senescence. Collectively, data from our previous study strongly supported the idea that, within 4 days, a single exposure to radiation could lead to the emergence of a prematurely senescent subpopulation of prostate cancer cells (13). Other studies suggest that senescent cells such as these have the potential to influence a tumor microenvironment through the secretion of soluble protumorigenic and antitumorigenic factors (3, 6, 8, 12, 15). However, the assortment of factors secreted seems to be cell type–specific and tissue-specific (12, 15). Senescent prostate fibroblasts have recently been shown to secrete soluble growth factors (3). Proteomic profiling of the soluble factors secreted by a variety of senescent cell types is currently a subject of intense investigation. However, we have found that the particulate material secreted by senescent prostate cancer cells may be equally informative.

Evidence of an endosomal origin for irradiation-induced exosome release. To establish a subpopulation of prematurely senescent cells, LNCaP and 22Rv1 cells were irradiated and allowed to accumulate over a period of 4 days before the medium was replenished with fresh serum-free medium and conditioned for 2 days, as previously described (13). Microvesicles secreted by these presenescent cells were isolated from the conditioned medium and the final fractions were examined by electron microscopy or stained using the lipid probe Vybrant DiI (21). Electron micrographs revealed that 22Rv1 cells released cup-shaped, rounded vesicles with a size of ~80 to 150 nm (Fig. 1*A*), similar to exosomes released by LNCaP prostate cancer cells (data not shown; ref. 18) and other cell types (18–20). Of note was the absence of any visual evidence of contamination by membrane fragments in our preparations of exosome-like particles. Additional evidence that microvesicles released by 22Rv1 cells were of endosomal origin is presented below (Fig. 1*B*).

Vybrant DiI was used as a sensitive fluorescent probe for measuring changes in the bulk level of microvesicles released by cells. The fluorescent intensity of these DiI-stained fractions were corrected for differences in the total number of viable cells left on each plate after the 48-hour conditioning period. The results of this assay provided evidence that the irradiation-induced senescence of 22Rv1 cells (13) was associated with an approximate 3-fold increase in the bulk level of microvesicles released by their unirradiated controls (Fig. 1*C*). These data indicate that irradiation therapy has the potential to induce a senescent phenotype associated with increased production and release of exosome-like particles into the microenvironment of neighboring cells that could potentially influence tumor progression.

We next used RNA interference to determine the cellular origin of the studied exosome-like particles. Two modes of exosome biogenesis have been described, immediate or delayed (22). The immediate mode of exosome biogenesis generates secreted vesicles that bud outward (i.e., away from the cytoplasm) from certain domains of the plasma membrane. This mode of exosome formation has been reported to be independent of class E vacuolar protein sorting function and MVEs (22). In contrast, the delayed mode of exosome biogenesis begins with outward vesicle budding at the limiting membrane of endosomes, generating MVEs. We targeted Tsg101 because this ubiquitin-binding protein is required for MVE vesicle formation (23) and a Tsg101 siRNA sequence had recently been shown to be effective in selectively decreasing the level of Tsg101 protein in PC3 prostate cancer cells (23). Four days after an exposure to mock, or 4 Gy irradiation, 22Rv1 cells were transfected with 100 nmol/L of Tsg101 siRNA and then incubated for an additional 3 days in antibiotic-free and serum-free medium.

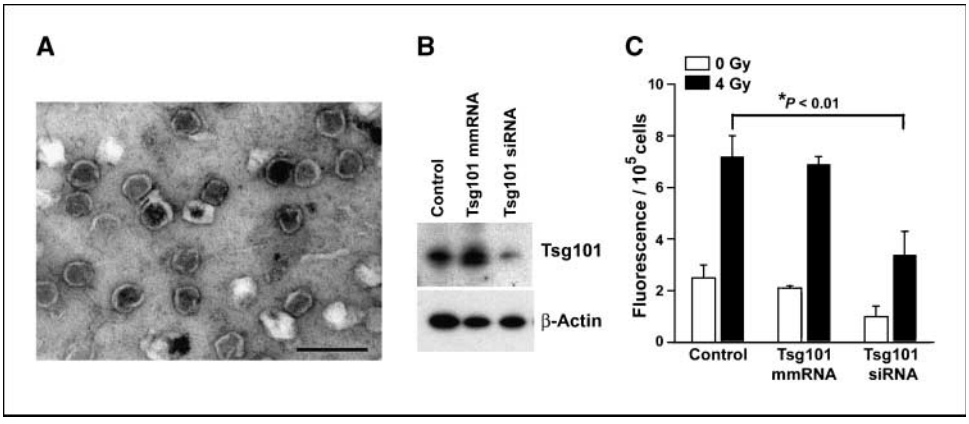

Figure 1. Ultrastructural and functional analysis of exosomes released from 22Rv1 prostate cancer cells. *A,* electron micrograph of 22Rv1 exosome-like particles. The image shows small cup-shaped vesicles of ~60 to 150 nm in diameter, which are representative of the exosome-like vesicles released by both 22Rv1 and LNCaP cells. Exosome fractions were isolated from serum-free medium conditioned by 22Rv1 cells for 48 h, beginning 4 d after irradiation (4 Gy). *Bar,* 200 nm. *B,* Western blot analysis of Tsg101 down-regulation in irradiated 22Rv1 cells. A mock transfection (*Control*) or transfection with a Tsg101 mismatch RNA (*mmRNA*) or Tsg101 siRNA (both 100 nmol/L) on day 3 after irradiation (4 Gy) was followed by harvesting of cell lysates on day 6. *C,* fluorescence assay of particulate membranes collected from medium conditioned on days 5 to 6 postirradiation. 22Rv1 cells were exposed to 0 or 4 Gy, incubated 4 d and transfected with Tsg101 mismatch RNA, siRNA, or untreated. After an additional 2 d, particulate fractions were isolated and stained. All values were then corrected for differences in viable cells left on the plate after 0 or 4 Gy. *Columns,* mean derived from two independent experiments done in triplicate; *bars,* SE; *, $P < 0.01$, Student's *t* test.

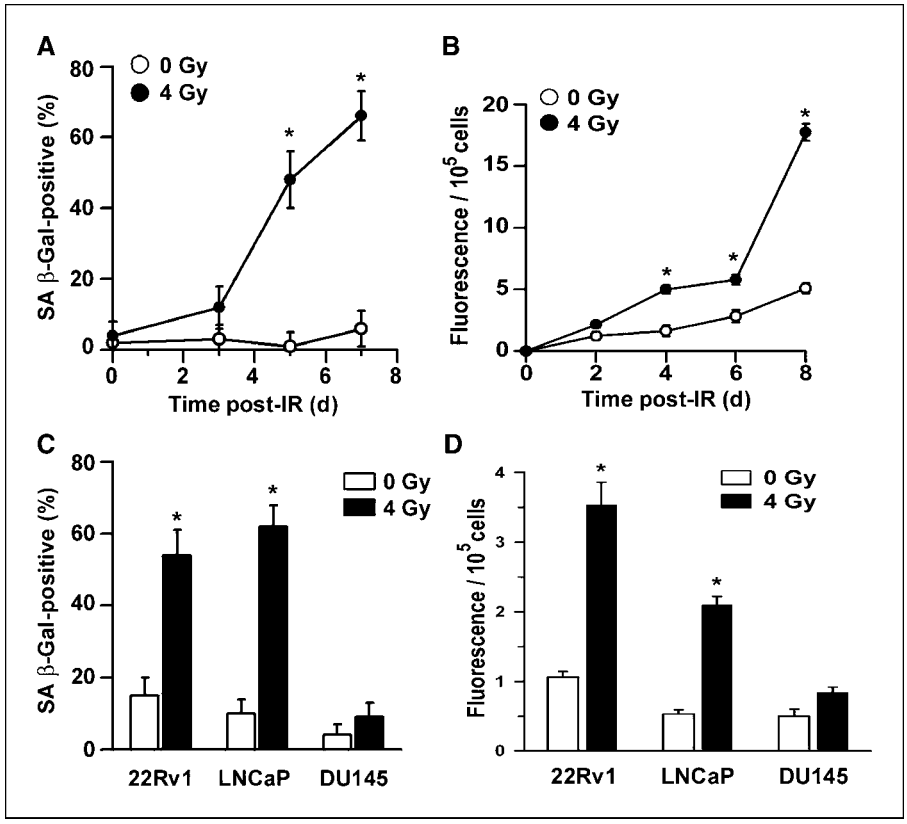

Figure 2. Senescence-associated release of exosomes from human prostate cancer cell lines. *A,* subconfluent cultures of 22Rv1 cells were exposed to either 0 Gy (mock control) or 4 Gy and, on the day specified, triplicate determinations of the percentage of SA β-Gal–positive cells were taken from a total of 300 cells in three independent experiments. *, $P < 0.01$, Student's *t* test. *B,* 22Rv1 cells were exposed to either 0 Gy (mock control) or 4 Gy and serum-free medium was conditioned 48 h during the intervals between 2 and 4, 4 and 6, 6 and 8, or 8 and 10 d after treatment. Exosome fractions were isolated from the conditioned medium and stained using Vybrant DiI. After normalizing for differences in cell survival, fluorescence intensity was plotted as a function of the time medium conditioning was initiated. *Points,* mean of three independent experiments done in triplicate; *bars,* SE; *, $P < 0.01$, Student's *t* test. *C,* LNCaP, 22Rv1, or DU145 cells were exposed to either 0 Gy (mock control) or 4 Gy, and on day 5 after irradiation, the percentage of SA β-Gal–positive cells was determined, as in *A*. *, $P < 0.01$, Student's *t* test. *D,* LNCaP, 22Rv1, or DU145 cells were exposed to either 0 Gy (mock control) or 4 Gy and serum-free medium was conditioned from 4 to 6 d after treatment. Exosome fractions were isolated from the conditioned medium and stained using Vybrant DiI. After normalizing for differences in cell survival, fluorescence intensity was plotted as a function of treatment condition and cell line tested. *Columns,* mean of triplicate determinations in two experiments; *bars,* SE. *, $P < 0.01$, Student's *t* test.

A 3-day exposure to Tsg101 siRNA resulted in an ~70% down-regulation at the protein level (ImageQuant TL; Fig. 1*B*) and ~55% reduction in basal exosome release in subconfluent cultures of proliferating 22Rv1 cells (i.e., unirradiated controls; Fig. 1*C*). Neither the mismatch RNA nor untreated control samples showed a significant change in Tsg101 protein levels or exosome release. Identical treatments with Tsg101 siRNA resulted in a 65% reduction in the extent to which irradiation-induced senescence was associated with an up-regulation of exosome release, when compared with the mismatch RNA and untreated controls (Fig. 1*C, filled columns*). Thus, electron microscopy and specific siRNA knockdown of Tsg101 provided significant evidence in favor of an endosomal/MVE origin for the vesicles under study.

p53-dependent and senescence-associated exosome release. A novel role for p53 in the control of intracellular protein trafficking has been proposed (8) and, more recently, it was shown that irradiation-induced activation of p53 can lead to significantly increased levels of exosome biogenesis and secretion by cultured human lung cancer cells (24). Moreover, there is evidence that the intrinsic MVE-exosomal transport pathway may be up-regulated in both ovarian cancer cells and erythroleukemic cells treated with the anticancer drug doxorubicin, which also activates a p53-dependent DNA damage response pathway (25, 26). Because prostate cancer cells also secrete exosome-like vesicles (18), we examined human prostate cancer cells for a potential functional relationship between irradiation-induced p53 activation, cellular senescence, and exosome secretion.

First, we analyzed conditioned medium from cultures of mock-treated (0 Gy) or irradiated (4 Gy) 22Rv1 cells for the presence of membrane vesicles at various times after treatment. Using SA β-Gal as an indicator of cellular senescence, the percentage of prematurely senescent 22Rv1 cells did not significantly increase within the 3 days following irradiation but had climbed to ~50% within 5 days postirradiation (Fig. 2*A*). Concurrent with this sharp increase in the relative number of prematurely senescent cells was an increase in the release of exosome-like vesicles from irradiated 22Rv1 cells (Fig. 2*B*). Beginning on the day specified, cultures were washed with PBS and incubated an additional 2 days in fresh serum-free medium to eliminate the possibility of any contamination by FBS-derived exosomes. The bulk level of particulate membrane which accumulated between 2 and 4 days after irradiation did not differ between mock controls and irradiated cultures. However, when the onset of conditioning was not initiated until the onset of premature cellular senescence (4 days postirradiation; ref. 13) there was a significantly greater amount of membrane vesicles accumulated in the medium conditioned by irradiated versus unirradiated 22Rv1 cells (Fig. 2*B*). This discrepancy remained evident, and grew, during the subsequent 4 days postirradiation (Fig. 2*B*).

Second, to determine whether this secretory pattern was restricted to senescent populations of prostate cancer cells, we compared the bulk levels of particulate membranes which accumulated between 4 and 6 days after cultured prostate cancer cells were exposed to either 0 or 4 Gy. A significant percentage of LNCaP and 22Rv1 cells become senescent within 4 days after irradiation (13), and there was a significant increase in the release of membrane vesicles associated with the irradiation-induced initiation of this cellular senescence (Fig. 2*C* and *D*). In contrast, DU145 cells neither display several of the phenotypic characteristics of a senescent cell nor increase in vesicle release following a single exposure to irradiation (Fig. 2*C* and *D*; ref. 13). Further evidence of a link between irradiation-induced p53 activation, premature senescence, and increased exosome release is presented

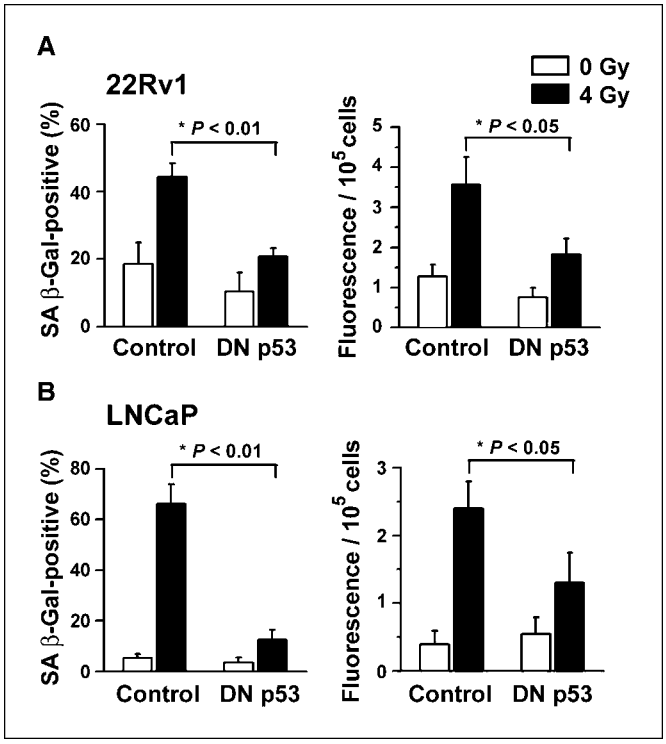

Figure 3. p53-dependent release of exosomes from prematurely senescent human prostate cancer cell lines. *A,* parental 22Rv1 cells and derivatives expressing a DN p53 mutant were exposed to either 0 or 4 Gy and on day 4 after irradiation (*left*) the percentage of SA β-Gal–positive cells was determined as in Fig. 2*A* or (*right*) cells were used to condition serum-free medium for 48 h. Exosome fractions were isolated from the conditioned medium and stained using Vybrant DiI. Fluorescence intensities were normalized for differences in cell survival. *Columns,* mean of two independent experiments done in triplicate; *bars,* SE. *B,* results of experiments conducted using LNCaP cells under identical conditions to those described in *A*.

in Fig. 3. Compared with their parental counterparts, fewer LNCaP and 22Rv1 cells transfected with a DN p53 mutant stained positive for SA β-Gal 4 days after irradiation and the observed differences in the release of exosome-like vesicles were diminished; each of these differences were statistically significant (Fig. 3). These data are consistent with the hypothesis that an increased biogenesis and/or release of exosome-like vesicles may comprise an important and previously unrecognized feature of premature cellular senescence.

Third, we tested the hypothesis that an increase in p53 activity would both enhance irradiation-induced cellular senescence and exosome secretion. To do this, we used nutlin-3, a small molecule antagonist of MDM2 that disrupts a negative feedback loop involving p53 ubiquitination (27). Nutlin-3 effectively primes the p53 pathway to respond to irradiation-induced DNA damage by increasing basal levels of p53 protein (Fig. 4*A*). Data shown in Fig. 4*B* summarize our recent findings (13) that MDM2 inhibition significantly decreases the clonogenic survival of LNCaP cells following a single exposure to the clinically relevant dose of 2 Gy (surviving fraction after 2 Gy = SF_2; Fig. 4*B*). Moreover, this radiosensitizing effect of nutlin-3 has previously been shown to be blocked by the expression of a DN p53 mutant (13) and could be entirely attributed to an increased induction of p53-dependent cellular senescence, rather than an increased percentage of apoptotic and necrotic cells (Fig. 4*B*). Finally, the introduction of nutlin-3 30 minutes prior to irradiation (4 Gy) and throughout the following 4 days resulted in a more than 2-fold increase in the release of exosome-like vesicles (Fig. 4*C*). This is the first investigation of the concept that p53 activity, premature senescence, and exosome biogenesis may be functionally coupled by intracellular signals and events that remain uncertain and represent important gaps in our current understanding of the secretory pattern of senescent cells.

To determine whether this secretory pattern was restricted to prematurely senescent populations of prostate cancer cells, we examined cultures of NHDF. NHDF cells have a finite life span *in vitro* and generally remain proliferative for less than 12 population doublings. When the bulk levels of particulate membranes released by proliferating and nonproliferating (i.e., senescent) cultures were

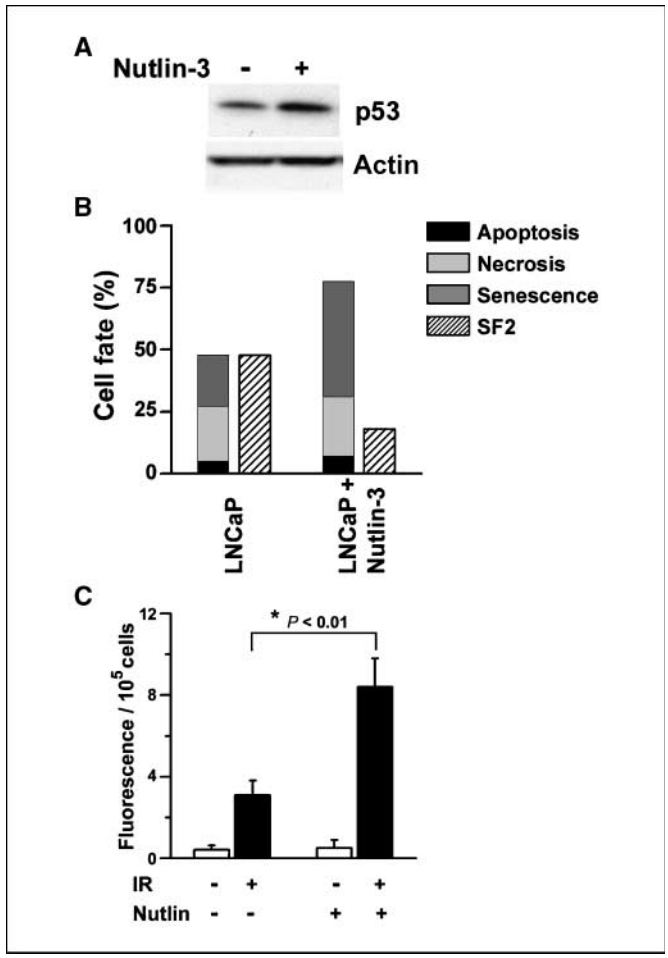

Figure 4. Nutlin-3–induced radiosensitization, premature senescence, and release of exosome-like particles. *A,* Western blot of p53 in whole cell lysates prepared from subconfluent cultures of LNCaP cells 48 h after the addition of 2 μmol/L of nutlin-3. The same lysates were also probed using an anti–β-actin antibody as a loading control. *B,* an overview of cell fate determinants (apoptosis, necrosis, senescence) in irradiated LNCaP cells at 48 h postirradiation (2 Gy). Data shown summarize the results of a previous study (13) and are the mean percentages of cells scored positive for apoptosis (i.e., using a combination of TdT-mediated dUTP nick end labeling, sub-G_1 DNA content, and acridine orange/ethidium bromide staining), necrosis (i.e., intact cells that failed to exclude ethidium bromide and displayed ethidium bromide–positive nuclei) or senescence (i.e., SA β-Gal and carboxyfluorescein diacetate succinimidyl ester flow cytometry) of triplicate determinations in two experiments. The fractions of cells surviving an exposure to 2 Gy (SF_2) were determined using clonogenic assays. Methods used to perform each of these assays have been described (13). *C,* LNCaP cells were incubated in the presence or absence of nutlin-3 (2 μmol/L) for 30 min and exposed to either 0 or 4 Gy. After an additional 4 d, particulate fractions were isolated and stained using Vybrant DiI. *Columns,* mean of two independent experiments done in triplicate; *bars,* SE; *, $P < 0.01$, Student's *t* test.

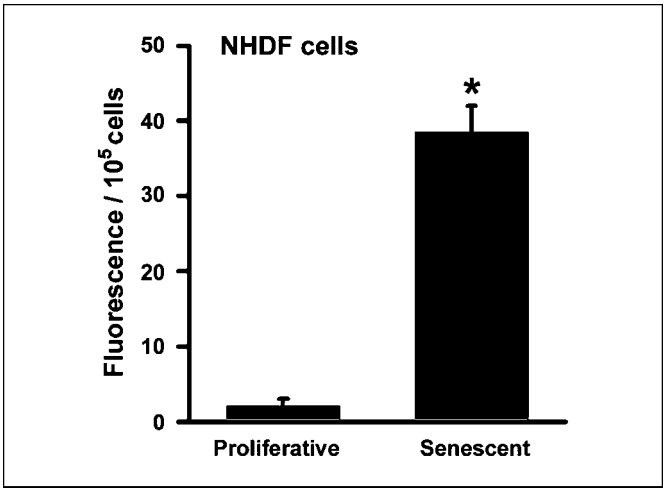

Figure 5. Proliferating (low passage) and nonproliferative (passage >10) cultures of NHDF cells were incubated for 48 h in the recommended medium containing 5% exosome-depleted FBS (i.e., post-100,000 × *g* supernatant). Exosome fractions were isolated from the conditioned medium and stained using Vybrant DiI. Fluorescence intensity is a function of lipid content, after normalizing for differences in cell survival. *Columns,* mean of triplicate determinations; *bars,* SE; *, $P < 0.01$, Student's *t* test.

compared, we observed a >15-fold increase in the release of exosome-like particles from NHDF cells that had naturally reached a state of replicative senescence (Fig. 5). These data provide strong support for the hypothesis that senescence, initiated either by telomere attrition (e.g., aging) or DNA damage (e.g., radiotherapy), may induce a p53-dependent increase in the biogenesis of exosome-like vesicles. This previously unrecognized feature of cellular senescence may hold important clues about the basic biology of both aging and the premature senescence of cancer cells.

Preliminary analysis of exosome cargo secreted by prematurely senescent prostate cancer cells. To determine whether irradiation-induced senescence was associated with qualitative, as well as quantitative, changes in MVE cargo sorting, we performed a SDS-PAGE analysis of the proteins associated with exosomal fractions collected from unirradiated and irradiated LNCaP and 22Rv1 cells. These assays showed that proteins detected in these gels were not derived from serum contamination of the exosome fractions (Fig. 6, *left, lane 4*) and confirmed that irradiation-induced senescence did not alter the overall profile of exosome proteins released (Fig. 6*A*). Moreover, comparisons of the proteins present in 22Rv1-derived whole cell lysates, exosome fractions, and soluble proteins indicated that exosomes were enriched in various subclasses of cellular proteins (Fig. 6, *right,* e.g., bands of ~13, 16, 30, 47, 58, 65, and 90 kDa). We have established that B7-H3 (CD276) represents one of the proteins enriched in the exosomes released by 22Rv1 cells (Fig. 6*B*). However, the presence of this protein has not been detected in exosomes released by LNCaP cells, possibly due to the relatively slow rate of exosome release from this cell line (Fig. 6*A*). In 22Rv1 cells, irradiation-induced senescence was associated with an increased release of B7-H3–positive exosomes that were free of contamination by cytosolic or mitochondrial proteins (e.g., ERK1/2 or cytochrome *C*; Fig. 6*C*); thus, providing independent confirmation of results obtained using DiI as a lipid probe to detect changes in exosome release. This is a novel and important finding, as B7-H3 is a member of the B7 family of proteins that are capable of modulating CD4 T-cell responses and antitumoral immunity (28–31). It was recently reported that increased B7-H3 expression provides an extremely reliable marker of prognosis for differentiating indolent from aggressive prostate cancers (32). The precise role of B7-H3 in prostate cancer and immunosurveillance has yet to be established. However, as a prognostic biomarker for aggressive cases of prostate cancer, B7-H3 has shown promise in immunohistochemical analyses of tissue sections (33). Because B7-H3 protein can be detected in the exosomes released by senescent 22Rv1 cells, it is possible that meaningful changes in the levels of circulating B7-H3–positive exosomes in the blood may provide a noninvasive way to survey the efficacy of radiotherapy for patients with prostate cancer.

Finally, we have extended the recent discovery by Valadi and colleagues (34) that exosomes contain small RNA. In this important study, the authors showed that exosomes released from mouse and human mast cells contain an abundance of small mRNAs and microRNAs (34). In addition, it was established that RNA from mouse mast cells was transferable to recipient human mast cells and can be translated after entering the recipient cell. In our preliminary analysis, we have found that prematurely senescent (irradiation-induced) 22Rv1 cells also release exosomes containing substantial amounts of small RNAs (Fig. 6*D*; <100 bp). To confirm that the nucleotides detected by agarose gel electrophoresis were RNA, exosome extracts were treated with either RNase or DNase in solution. The results showed minimal degradation by DNase, whereas added RNase degraded exosome RNA and revealed the presence of a single DNA band of >1,000 bp (Fig. 6*D*). The studies described here present the challenges of addressing the basic questions of whether the RNA cargo contained in MVE-derived exosomes are generically capable of mediating cell-cell communication, as in the case of human mast cells (34), and to investigate the mechanisms of "exosomal shuttle RNA" uptake by neighboring cells.

Clinically relevant doses of irradiation induce a premature state of cellular senescence that accounts for most of the clonogenic death observed in cultures of human prostate cancer cells retaining a functional p53 DNA damage-response pathway (13). We show here for the first time that this treatment-induced cell cycle arrest was associated with a senescence-associated increase in exosome release. In accelerated senescence, this novel secretory phenotype was dependent on the activation of p53. However, the release of exosome-like microvesicles also increased during proliferative senescence in normal human fibroblasts. This suggests that senescence, initiated either by telomere attrition (e.g., aging) or DNA damage (e.g., radiotherapy), may induce a p53-dependent increase in the biogenesis of exosome-like vesicles. Ultrastructural analysis and RNA interference–mediated knockdown of Tsg101 provided significant evidence that the additional exosomes released by prematurely senescent prostate cancer cells were principally derived from MVEs. Moreover, these exosomes were enriched in B7-H3 protein, a recently identified diagnostic marker for prostate cancer and an abundance of exosomal shuttle RNA. Many details regarding the mechanisms that control exosome biogenesis and their potential role in intercellular communication remain obscure. Our findings are consistent with the proposal that exosomes can transfer cargos, with both immunoregulatory potential and genetic information, between cells through a novel mechanism that may be recruited to increase exosome release during treatment-induced and replicative cellular senescence.

Disclosure of Potential Conflicts of Interest

No potential conflicts of interest were disclosed.

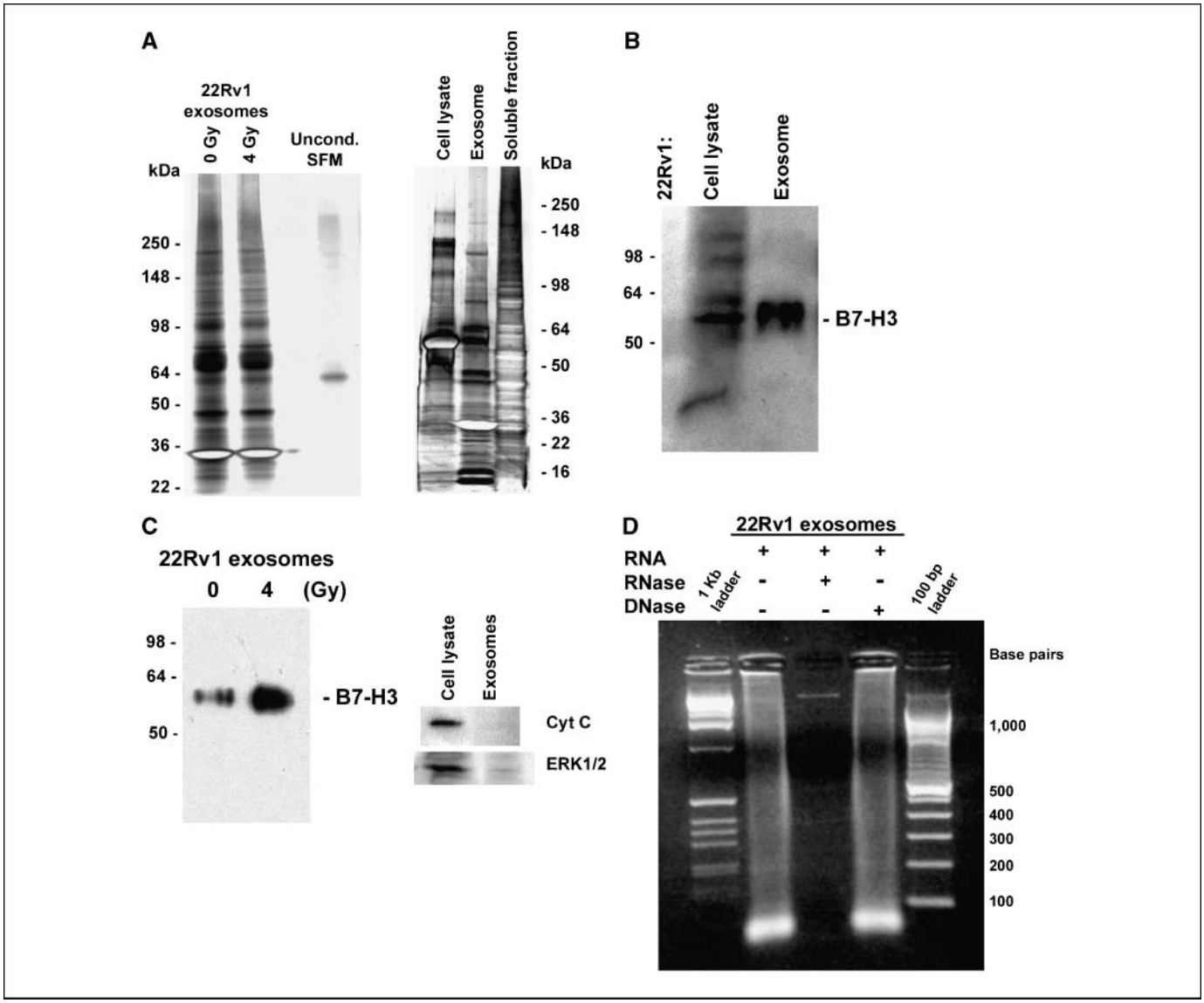

Figure 6. Secretion patterns of human prostate cancer cells. *A,* silver staining analysis of the exosome fractions released, 4 to 6 d after exposure to either 0 or 4 Gy, by 22Rv1 cells. *Left,* electrophoresis was performed on 8% to 16% Tris-glycine gels; lane 4 is a negative control loaded with unconditioned serum-free medium (*Uncond. SFM*). *Right,* comparison of the silver-stained protein profiles for 22Rv1 total cell lysates, exosome fractions, and exosome-free medium (*Soluble fraction*) conditioned 4 to 6 d after irradiation (4 Gy). Electrophoresis was performed on 4% to 20% gels. *B,* Western blot analysis of B7-H3 protein in a whole cell lysate and exosome fraction isolated from medium conditioned 48 h by irradiated 22Rv1 cells. *C,* Western blot analysis of B7-H3 protein in exosome fractions and an absence of contamination by either cytochrome *C* or ERK1/2. Exosomes were isolated 4 d after the exposure of 22Rv1 cells to either 0 or 4 Gy; total cell lysates were prepared from remaining adherent cells. Final exosome pellets were resuspended in equal volumes of lysis buffer and 20% of the total volumes for each sample were loaded. The position of molecular weight markers (in kDa; *left*). *D,* large amounts of small RNA (<100 bp) were detected in 22Rv1-derived exosomes on a 2% agarose gel stained by ethidium bromide; treatments with either RNase or DNase confirmed the presence of both DNA and RNA.

Acknowledgments

Received 12/7/2007; revised 7/14/2008; accepted 7/16/2008.

Grant support: NIH grant R01CA098195 (J.A. McCubrey) and the Brody Brother's Foundation Endowment no. 997729 (D.M. Terrian and J.A. McCubrey).

The costs of publication of this article were defrayed in part by the payment of page charges. This article must therefore be hereby marked *advertisement* in accordance with 18 U.S.C. Section 1734 solely to indicate this fact.

We thank Warren Knudson for the NHDF cells and members of the Anatomy and Cell Biology Workshop Series for their many helpful suggestions.

References

1. Cooperberg MR, Broering JM, Litwin MS, et al. CaPSURE Investigators. The contemporary management of prostate cancer in the United States: lessons from the cancer of the prostate strategic urologic research endeavor (CapSURE), a national disease registry. J Urol 2004;171:1393–401.
2. Hayflick L, Moorhead PS. The serial cultivation of human diploid cell strains. Exp Cell Res 1961;25:585–621.
3. Bavik C, Coleman H, Dean JP, Knudsen B, Plymate S, Nelson PS. The gene expression program of prostate fibroblast senescence modulates neoplastic epithelial cell proliferation through paracrine mechanisms. Cancer Res 2006;66:794–802.
4. Chang B-D, Watanabe K, Broude EV, et al. Effects of $p21^{Waf1/Cip1/Sdi1}$ on cellular gene expression: implications for carcinogenesis, senescence, and age-related diseases. Proc Natl Acad Sci U S A 2000;97:4291–6.
5. Krtolica A, Parrinello S, Lockett S, Desprez PY, Campisi J. Senescent fibroblasts promote epithelial cell growth and tumorigenesis: a link between cancer and aging. Proc Natl Acad Sci U S A 2001;98:12072–7.

6. Coppe J-P, Kauser K, Campisi J, Beausejour CM. Secretion of vascular endothelial growth factor by primary human fibroblasts at senescence. J Biol Chem 2006;281:568–74.
7. Currid CA, O'Connor DP, Chang BD, et al. Proteomic analysis of factors released from p21-overexpressing tumour cells. Proteomics 2006;6:3739–53.
8. Khwaja FW, Svoboda P, Reed M, Pohl J, Pyrzynska B, Van Meir EG. Proteomic identification of the wt-p53-regulated tumor cell secretome. Oncogene 2006;25:7650–61.
9. Olumi AF, Grossfeld GD, Hayward SW, Carroll PR, Tisty TD, Cunha GR. Carcinoma-associated fibroblasts direct tumor progression of initiated human prostatic epithelium. Cancer Res 1999;59:5002–11.
10. Chen Z, Trotman LC, Shaffer D, et al. Crucial role of p53-dependent cellular senescence in suppression of Pten-deficient tumorigenesis. Nature 2005;436:725–30.
11. Roninson IB. Oncogenic functions of tumour suppressor p21(Waf1/Cip1/Sdi1): association with cell senescence and tumour-promoting activities of stromal fibroblasts. Cancer Lett 2002;179:1–14.
12. Campisi J. Suppressing cancer: the importance of being senescent. Science 2005;309:886–7.
13. Lehmann BD, McCubrey JA, Jefferson HS, Paine MS, Chappell WH, Terrian DM. A dominant role for p53-dependent cellular senescence in radiosensitization of human prostate cancer cells. Cell Cycle 2007;6:595–605.
14. Roninson IB. Tumor cell senescence in cancer treatment. Cancer Res 2003;63:2705–15.
15. Shay JW, Roninson IB. Hallmarks of senescence in carcinogenesis and cancer therapy. Oncogene 2004;23:2919–33.
16. Taylor DD, Gercel-Taylor C. Tumour-derived exosomes and their role in cancer-associated T-cell signaling defects. Br J Cancer 2005;92:305–11.
17. Keller S, Sanderson MP, Stoeck A, Altevogt P. Exosomes: from biogenesis and secretion to biological function. Immunol Lett 2006;07:102–8.
18. Abusamra AJ, Zhong Z, Zheng X, et al. Tumor exosomes expressing Fas ligand mediate CD8+ T-cell apoptosis. Blood Cells Mol Dis 2005;35:169–73.
19. Fevrier B, Raposo G. Exosomes: endosomal-derived vesicles shipping extracellular messages. Curr Opin Cell Biol 2004;16:415–21.
20. Thery C, Regnault A, Garin J, et al. Molecular characterization of dendritic cell-derived exosomes. Selective accumulation of the heat shock protein hsc73. J Cell Biol 1999;147:500–10.
21. Sengupta P, Holowka D, Baird B. Fluorescence resonance energy transfer between lipid probes detects nanoscopic heterogeneity in the plasma membrane of live cells. Biophys J 2007;92:3564–74.
22. Razi M, Futter CE. Distinct roles for Tsg101 and Hrs in multivesicular body formation and inward vesiculation. Mol Biol Cell 2006;17:3469–83.
23. Zhu G, Gilchrist R, Borley N, et al. Reduction of TSG101 protein has a negative impact on tumor cell growth. Int J Cancer 2004;109:541–7.
24. Yu X, Harris SL, Levine AJ. The regulation of exosome secretion: a novel function of the p53 protein. Cancer Res 2006;66:4795–801.
25. Chen VY, Posada MM, Blazer LL, Zhao T, Rosania GR. The role of the VPS4A-exosome pathway in the intrinsic egress route of a DNA-binding anticancer drug. Pharm Res 2006;23:1687–95.
26. Shedden K, Xie XT, Chandaroy P, Chang YT, Rosania GR. Expulsion of small molecules in vesicles shed by cancer cells: association with gene expression and chemosensitivity profiles. Cancer Res 2003;63:4331–7.
27. Vassilev LT, Vu BT, Graves B, et al. *In vivo* activation of the p53 pathway by small-molecule antagonists of MDM2. Science 2004;303:844–8.
28. Booth AM, Fang Y, Fallon JK, Yang JM, Hildreth JE, Gould SJ. Exosomes and HIV Gag bud from endosome-like domains of the T cell plasma membrane. J Cell Biol 2006;172:923–35.
29. Wang LQ, Fraser CC, Kikly K, et al. B7-3 promotes acute and chronic allograft rejection. Eur J Immunol 2005;35:428–38.
30. Suh WK, Gajjewska BU, Okada H, The B7 family member B7-3 preferentially down-regulates T helper type 1-mediated immune responses. Nat Immunol 2003;4:899–906.
31. Prasad DV, Nguyen T, Li Z, et al. Murine B7-3 is a negative regulator of T cells. J Immunol 2004;173:2500–6.
32. Roth TJ, Sheinin Y, Lohse CM, et al. B7-3 ligand expression by prostate cancer: a novel marker of prognosis and potential target for therapy. Cancer Res 2007;67:7893–900.
33. Steinberger P, Majdic O, Derdak SV, et al. Molecular characterization of human 4Ig-B7-3, a member of the B7 family with four Ig-Like domains. J Immunol 2004;172:2352–9.
34. Valadi H, Ekstrom K, Bossios A, Sjostrand M, Lee JJ, Lotvall JO. Exosome-mediated transfer of mRNAs and microRNAs is a novel mechanism of genetic exchange between cells. Nat Cell Biol 2007;9:654–9.